

Study on the impact of blades wrap angle on the performance of pumps as turbines used in water supply system of high-rise buildings

Ji Yun Du, Hongxing Yang* and Zhicheng Shen

Renewable Energy Research Group (RERG), Department of Building Services Engineering,
The Hong Kong Polytechnic University, Hung Hom, Kowloon, Hong Kong, China

Abstract

The use of pumps as turbines (PATs) in different applications has attracted increasing attention in recent years. Based on our previous research, the PAT could be used in water supply system of high-rise buildings for water head reduction and hydropower generation, but the efficiency is relatively low. Due to the high water head and low flow rate, PATs used in water pipelines are usually low specific speed turbines. According to the impeller inlet and outlet velocity triangles, the blades wrap angle of a centrifugal pump is not optimal for low specific speed turbines, so the impact of blades wrap angle on the PAT performance should be studied. In this paper, the impact is investigated by numerical and experimental methods. Firstly, a 3D model of an original PAT was built in CAD software, then the model was imported into the ICEM to generate grids and then imported into Ansys CFX for simulation. After simulation, a PAT prototype was tested in the lab test rig to validate the simulation results. The comparison between simulation and experimental results indicates that although some deviations exist, the simulation could provide an acceptable prediction of the PAT's performance. Finally, four PAT models with different blades wrap angles were developed to compare their performance in terms of both power output and water head reduction. The results show that the blades wrap angle does have effects on the PAT's efficiency and hydraulic loss, to achieve a good balance between water head reduction and power output. The model with -60° wrap angle has the best performance.

Keywords: pump as turbines; blades wrap angle; water supply system; high-rise buildings

*Corresponding author: Received 10 November 2017; revised 21 December 2017; editorial decision 29 December 2017; accepted
Hong-xing.yang@polyu.edu.hk 2 January 2018

1 INTRODUCTION

In recent decades, the pump as turbine (PAT) has attracted increasing attention in remote micro hydropower generation and industry hydropower recovery due to its low cost, easy maintenance and easy access in the market [1, 2]. In our former research, the feasibility of micro hydropower generation in the water supply system of high-rise buildings using the PAT has been studied by both numerical and experimental methods. The results showed that the PAT has a good performance in electricity generation as well as water head reduction. However, the results also indicated that efficiency of the PAT used in the water supply pipeline, which is characterized by high water head and low flow rate, is relatively low [3]. Therefore, it is an

important topic in PAT investigation to improve the PAT's efficiency.

Many researchers have attempted different techniques to improve the PAT efficiency. Among them, some investigators put their attention on the PAT geometry modification or optimization for performance improvement. Yang [4] proposed a PAT's volute design method to optimize the volute shape for PAT performance enhancement. In the study of D.R. Giosio [1], the volute of one commercially available pump is modified for incorporation of inlet flow control, experimental results showed that the customized PAT has a wider range of high efficiency operation than the parent pump. Baoshan Zhu [5] conducted optimization design on the PAT blades based on 3D inverse design, computational fluid mechanics (CFD) and lab tests, this study proved that the blades

shape optimization could improve the PAT performance with high efficiency and operation stability. The research of several investigators paid the focus on the effect of blades, hub and shroud rounding on PAT efficiency, the results showed that the rounding of blades, hub and shroud could lead to 1–3% efficiency increase [6–8]. Besides, impeller trimming can lead to efficiency improvement at part load operating conditions [8].

According to the design principle of turbomachine blades, the original blades shape of the pump is designed to provide sufficient power to the water. But when a pump operates in reverse as a turbine in a working condition of high water head [9]. Yang [10] investigated the influence of blades wrap angle on the PAT performance by numerical and experimental methods, but this research only focused on the back curved blades, the effects of forward curved with different wrap angles on the PAT performance still lacks.

In the present paper, the effects of different wrap angles on the PAT performance was studied by numerical and experimental methods. Firstly, the CAD model of the original PAT was built and imported into ICEM for meshing, then CFD simulation was conducted in Fluent. Thereafter, the prototype of the PAT was tested in the hydraulic test rig to validate the simulated results. After that, another three PAT models with different blades curving degree were built and simulated to compare the performance in output power, efficiency and water head reduction.

2 METHODOLOGY

In recent years, CFD technology has been a successful and mature way in aspects of PAT inner flow analysis, performance prediction and optimization [11–13]. In the present research, numerical simulation and lab experiments are used to study the effect of different blades wrap angles on the performance of the PAT. The models of PATs with different blades wrap angles were built in Solidworks, these models were then imported into ANSYS ICEM and FLUENT for meshing and simulation, respectively. The PAT prototype with original blades was tested in the hydraulic test rig for performance study and validation of simulations.

2.1 Geometric parameters

This study aims to study the effects of blades wrap angle on the PAT performance, so in all the models, the main geometric parameters (as listed in Table 1) keep constant except the blades wrap angle. The CAD models of four different blades are shown in Figure 1. To identify these four different models, the blades wrap angle of original model is regarded as positive value, that is 120° (Figure 1a), and blades wrap angles of another three models are regarded as 60° (Figure 1b), -60° (Figure 1c) and -120° (Figure 1d), respectively.

2.2 CFD setting

2.2.1 Meshing

The PAT physical model, which is composed of four main parts: inlet reducer, volute, impeller and outlet reducer, were built in

Table 1. Geometric parameters of PAT.

Parameters	Values
Impeller Inlet Diameter (mm)	160
Impeller Outlet Diameter (mm)	40
Impeller Width (mm)	4
Impeller Blade Thickness (mm)	5
Volute Base Circle Diameter (mm)	170
Volute Inlet Diameter (mm)	25
Volute Outlet Diameter (mm)	25
Blades Number	5

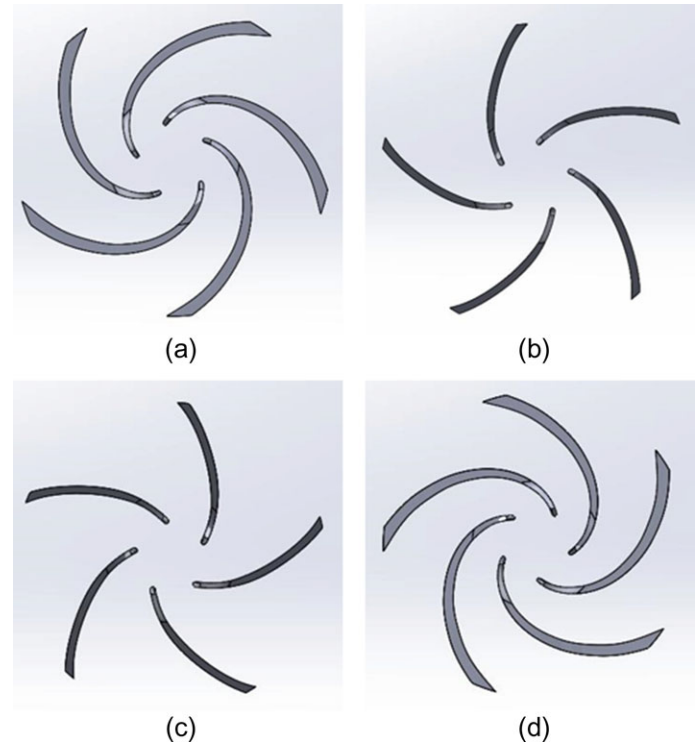


Figure 1. CAD models of blades with different curving degree.

SolidWorks, a three-dimensional modeling computer-aided design software. Then the physical model was imported into ICEM-CFD for unstructured tetrahedral grids generation. The whole computational domain was separated into two main domains: stationary domain and rotary domain. Inlet reducer, volute and outlet reducer belong to the stationary domain while impeller is the rotary domain. For simulation, the sliding-mesh interface method was adopted to allow for the mesh motion between static and rotating parts [14, 15]. In the meshing process, the ‘tetra mesh’ was employed to generate grids in the domains far from boundaries, while the ‘prism mesh’ was used for grid generation in the domains near boundaries, i.e. the pipe wall and volute wall. Such strategy could achieve a good balance between calculation time and accuracy. As shown in Figure 2 is the final computational mesh and the total mesh number is about 2.01 million, which is considered well enough for such a small computational domain

based on our former research [3], so investigation of the grid-dependence is unnecessary.

2.2.2 Solver setup

The incompressible isothermal flow through a turbomachine is fully described by the continuity and momentum equations, which are called the Navier–Stokes equations and written as:

$$\frac{\partial u_i}{\partial x_i} = 0, \quad (1)$$

$$\frac{\partial u_i}{\partial t} + u_j \frac{\partial u_i}{\partial x_j} = -\frac{1}{\rho} \frac{\partial p}{\partial x_i} + \nu \frac{\partial^2 u_i}{\partial x_i \partial x_i}, \quad (2)$$

where u is the velocity, p is the pressure, ν is the kinematic viscosity of fluid, ρ is the fluid density.

Since solving the Navier–Stokes equations is computationally expensive for high Reynolds number flows in complex geometries, the Reynolds averaged Navier–Stokes (RANS) equations are generally solved to determine the mean velocity field. RANS equations are obtained by time-averaging the Navier–Stokes equations for the mean values of the flow variables over a sufficiently long period compared to the frequencies of turbulent fluctuations, and are written as:

$$\frac{\partial u_i}{\partial x_i} = 0, \quad (1)$$

$$\frac{\partial U}{\partial t} + U_j \frac{\partial U_i}{\partial x_j} = -\frac{1}{\rho} \frac{\partial P}{\partial x_i} + \frac{\partial}{\partial x_j} \left[\nu \left(\frac{\partial U_j}{\partial x_i} + \frac{\partial U_i}{\partial x_j} \right) - \overline{u'_i u'_j} \right], \quad (4)$$

where U is the time-averaged velocity, u'_i is the fluctuating velocity due to turbulence and $-\rho \overline{u'_i u'_j}$ is the Reynolds shear stress.

RANS simulations with appropriate turbulence models have been widely used for turbomachinery design analyses due to their low computational cost and satisfactory predictive capability for average device performance [16, 17]. Based on our

former research [3], the SST $k - \omega$ model may be more accurate and reliable than $k - \varepsilon$ model in PAT performance prediction because the SST $k - \omega$ model combines the standard $k - \omega$ model and standard $k - \varepsilon$ model, it takes the effects of turbulence shear stress into consideration in the definition of the turbulence viscosity and could capture the micro flow in the viscous layer. In this paper, the SST $k - \omega$ model was used to combine with the RANS approach for CFD simulations.

2.2.3 Boundary conditions

Figure 3 shows the schematic diagram of real model and CFD model of the investigated PAT. In the real model, water leakage exists in the space between impeller hub/shroud and casing, which means the actual flow rate through the impeller is less than that under working condition [18]. However, in the study, leakage could not be simulated because the numerical model did not include the flow field of leakage. To obtain a more accurate simulation results, the leakage is estimated as a function of the geometry of the flow field and the head [19]:

$$Q_L = (A_f + A_b) H_m^{0.5}, \quad (5)$$

$$A = \frac{\pi \sqrt{2g} \mu \left(\frac{2cl}{D_s} \right) \left(\frac{\Delta H_{cl}}{H_m} \right)^{0.5} D_0^2}{2 \left(\frac{D_0}{D_s} \right)^2 \left(1 - \left(\frac{D_h}{D_0} \right)^2 \right)}, \quad (6)$$

$$D_{sf} = 1.29 D_0, \quad (7)$$

$$D_{sb} = 1.32 D_0, \quad (8)$$

where Q_L is the leakage flow (m^3/h), H_m is the design head (m), A_f and A_b are the areas of fore and back leakage passage, respectively (m^2), μ is the leakage flow coefficient which is assumed 0.4, cl is the size of the seal clearance which is set to 0.00015, $\Delta H_{cl}/H_m$ is the coefficient of head loss through the seal, which is assumed 0.75, D_s represents the annular gap diameter of the seal (m), D_0 is the eye diameter of impeller (m), D_h is the hub diameter (m).

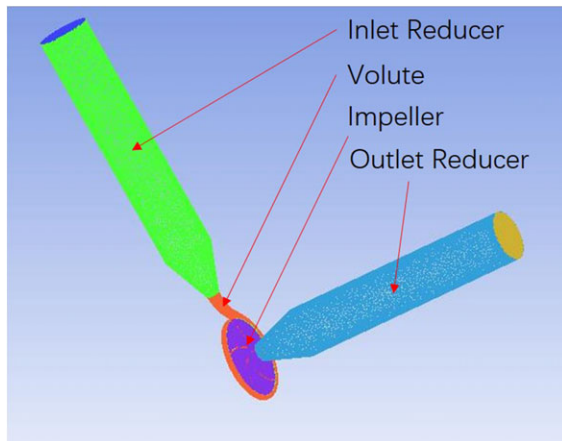


Figure 2. The final meshing scheme.

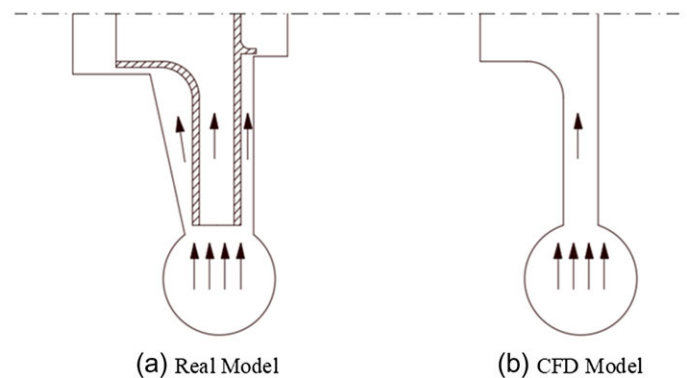


Figure 3. Schematic diagram of PAT model.

To obtain more reliable simulation results, the water leakage estimated by the above equations is reduced from the inlet discharge at the inlet boundary. The inlet velocity is considered as the inlet boundary condition of the inlet face while the outlet boundary condition is set as pressure outlet with the pressure equal to atmospheric pressure. Besides, the boundary condition of turbine wall and blades is set as rough wall with the roughness $100\mu\text{m}$ and the root mean square (RMS) residual is set to 10^{-5} .

2.3 Experimental setup

To validate the results of simulation, a PAT prototype with the 100% curving degree was purchased and tested in the hydraulic test rig in the laboratory of the Renewable Energy Research Group at The Hong Kong Polytechnic University. Figure 4 shows the schematic diagram of the hydraulic test rig, which is composed of a water tank, a power pump, control valves, flow meters and pressure sensors. The power pump is a commercial centrifugal pump controlled by a frequency converter. The maximum water head and flow rate of the power pump is 82 m and $81\text{ m}^3/\text{h}$, respectively, by adjusting the frequency of motor, the water head and flow rate could be adjusted accordingly to provide a needed working condition. Besides, two pressure sensors were used to examine the pressure drop between the upstream and downstream of the PAT and one electromagnetic flowmeter was adopted for the flow rate measurement in the pipeline, all the sensors and flowmeter are located far from the PAT for accurate measurement. A 24 V three-phase permanent magnet alternating generator with low starting torque was chosen to translate shaft power of the PAT into electric energy, after rectification in the controller, the electricity was stored in two lead acid batteries and the power and voltage output could be obtained from the controller.

2.4 Data analysis

To assess the turbine performance, both the numerical and experimental output power and water head reduction should be monitored. The experimental results can be obtained directly by measuring the generator power and collecting the data from pressure meters. However, some calculation is necessary to get

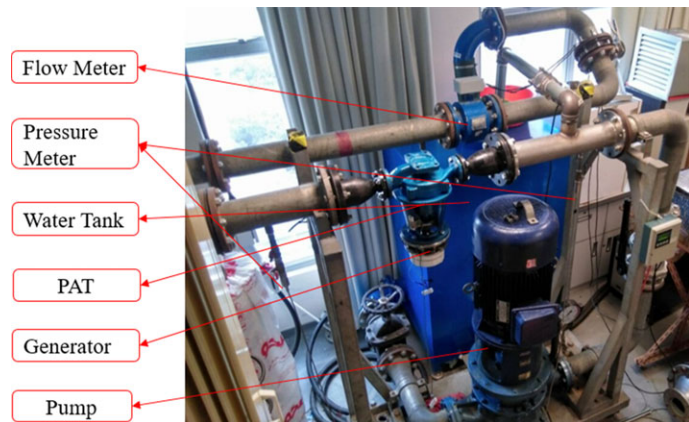


Figure 4. The schematic diagram of the hydraulic test rig.

the numerical results that corresponding to the experimental results. In the CFD simulation, the output torque of the impeller is recorded and the shaft power of the turbine is calculated by Equation (9). For the calculation of output power, mechanical loss and generator conversion efficiency must be considered as energy loss is inevitable in energy conversion process, as shown in Equation (10):

$$P_{\text{shaft}} = T\omega, \quad (9)$$

$$P_s = \eta_{\text{me}} \eta_g P_{\text{shaft}}, \quad (10)$$

where P_{shaft} is the shaft power (W), ω is the rotational speed (rad/s), T is the shaft torque (N·m), P_s is the actual simulation power output (W), η_{me} is the overall mechanical efficiency and η_g is the conversion efficiency of generator. In this study, the mechanical efficiency and generator conversion efficiency are determined based on the data provided by parts suppliers.

Besides, as the CFD model is simplified and leakage is reduced in the simulation process, the water head loss caused by water leakage needs to be estimated and added to the simulated water head. The head reduction caused by leakage, H_L , is estimated by the empirical formula developed by Stepanoff [20]:

$$H_L = \frac{3}{4} \frac{u_1^2 - u_2^2}{2g}, \quad (11)$$

where u_1 and u_2 are the inlet and outlet tangential velocities of the impeller (as is shown in Figure 6) and they can be calculated as a function of the rotation speed and diameter:

$$u_1 = \frac{\pi D_1 N}{60}, \quad (12)$$

$$u_2 = \frac{\pi D_2 N}{60}, \quad (13)$$

where D_1 and D_2 are the diameters of inlet and outlet of the impeller, respectively (m), N is the rotation speed of the PAT (rpm).

3 RESULTS AND ANALYSIS

As the customization of impeller prototypes is very difficult and costly, so in this research, only the prototype of original impeller, of which the blades wrap angle is 120° , was purchased and tested in the lab test rig. After lab tests, the experimental results are used to validate the simulation results of the corresponding PAT model. Finally, the comparison between the simulation results of four different PAT models to study the effects of blades curving degree on the PAT performance.

3.1 Validation of numerical simulation

After a series of simulations and lab tests, the numerical and experimental performance curves of the PAT with 120° blades wrap angle were achieved. To compare the numerical and

experimental results, mechanical losses in mechanical seal, mechanical transmission components and generator, which are provided by the pump and generator manufacturer, are reduced from the simulated output power and efficiency.

The experimental and simulation results of model with 120° blades wrap angle are shown in Figures 5 and 6. It can be noticed that both the best efficiency points (BEPs) of experimental and simulation results are located at 10 m³/h. For experimental results, the best efficiency is 11.7% with 113 W power generated and 35 m water head reduced, while for simulation results, the best efficiency is 12.8% with 106 W power generated and 30 m water head reduced.

However, it can also be observed that there are some deviations between CFD results and experimental results, the difference in efficiency, power output and water head reduction is about 1.1%, -7 W and 5 m, respectively, at the BEP. These

deviations have also been confirmed by other published numerical research [21]. There are two main reasons for this quantitative difference. On the one hand, the simplicity of CFD model may cause miscalculation on the hydraulic loss, but this miscalculation is difficult to be measured and ruled out. Besides, water in the space between impeller hub/shroud and casing results in severe disc friction, which reduces the conversion efficiency from hydropower to mechanical shaft power significantly. The effect of disc friction loss is likely to be greater in low specific speed turbines, however, it could not be simulated in this study because the numerical model did not include the flow field between impeller hub/shroud and casing.

Regardless of the difference between numerical and experimental results, the trends and BEP locations of the simulated results are consistent with that of the testing results from the qualitative point of view. The numerical results do provide important and acceptable prediction of the PAT performance.

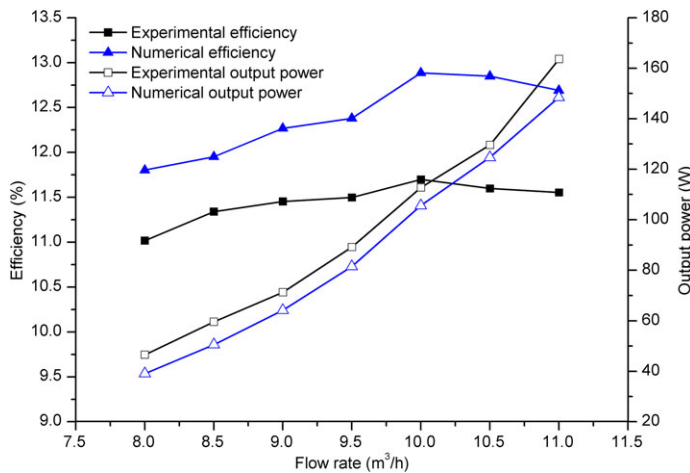


Figure 5. The comparison between experimental and numerical efficiency and output power.

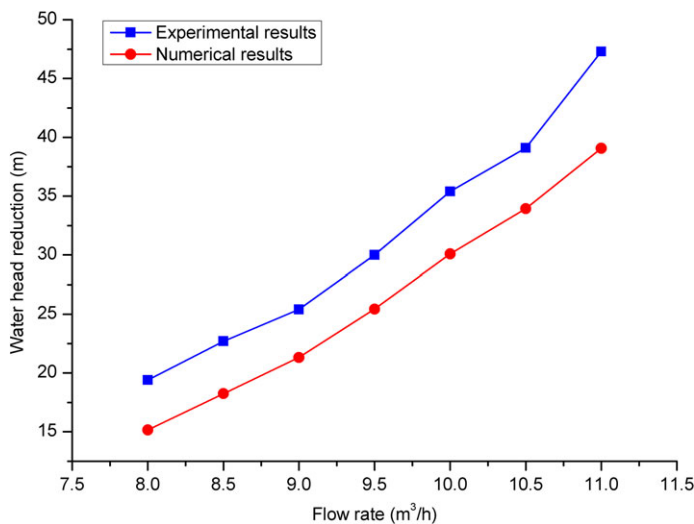


Figure 6. The comparison between experimental and numerical water head reduction.

3.2 Output power and efficiency

As the main purpose of using the PAT in water supply system of high-rise building is to reduce water head and to generate electricity, the simulated water head reduction and output power are set as the parameters for performance assessment. Figures 7 and 8 show the performance curves of models with different blades wrap angle. Figure 7 indicates that the best efficiency of the PAT increases from 12.9% to 16.0% by changing the blades wrap angles and the maximum efficiency occurs when the blades wrap angle is -60°. Besides, it can also be observed that flow rates at the BEPs varies with the change of blades wrap angle. Figure 8 shows that the model of -60° wrap angle generates the maximum output power while the model of 60° wrap angle has the poorest power generation. The main reason for this performance difference is that changing the blades wrap angle leads to the variation of flow attack angle, resulting in different impact loss in the impeller. In conclusion,

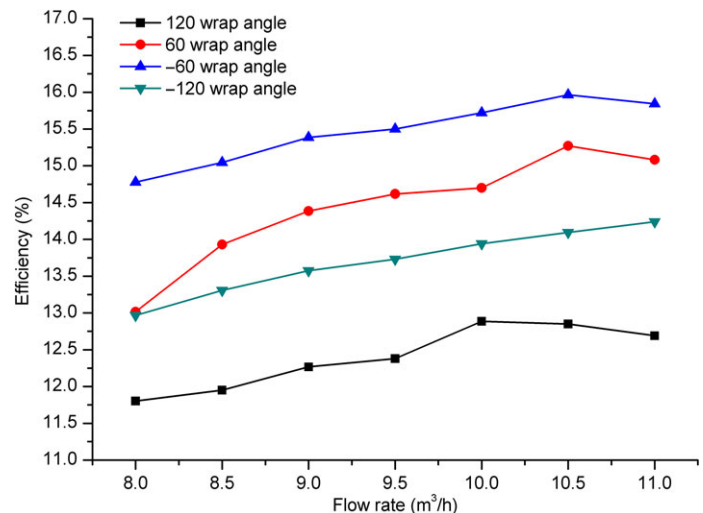


Figure 7. Efficiency comparison between different PAT models.

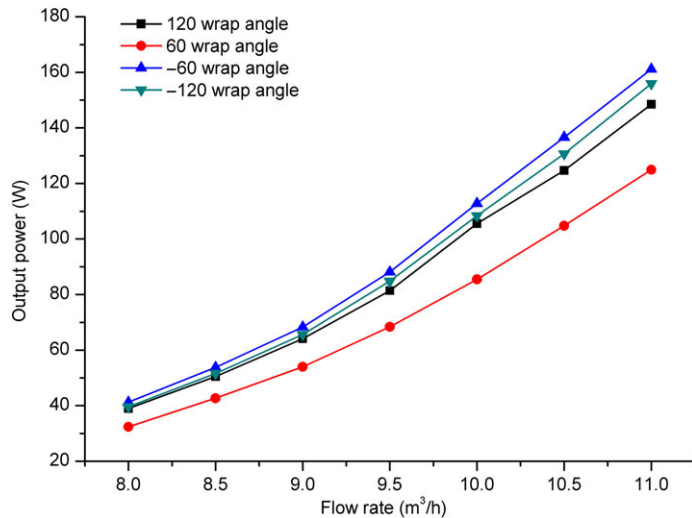


Figure 8. Output power comparison between different PAT models.

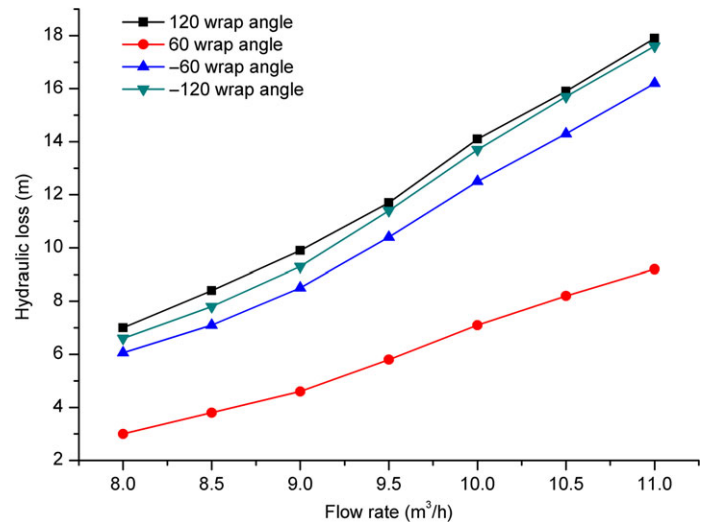


Figure 10. Hydraulic loss in impeller of PAT models.

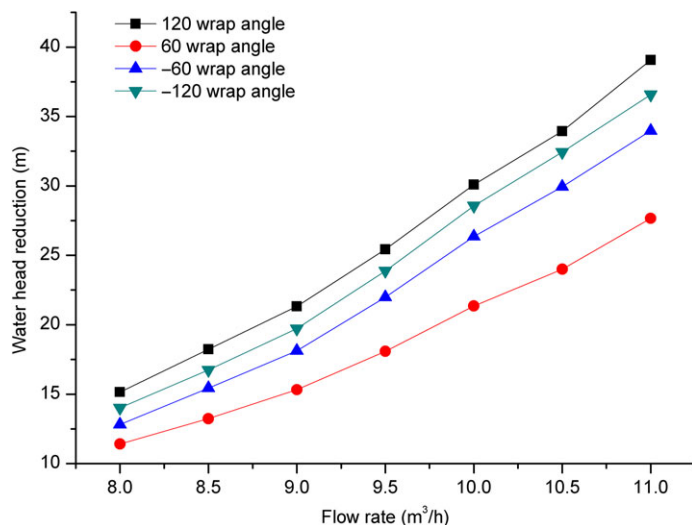


Figure 9. Water head reduction of different PAT models.

in terms of efficiency and power output, the model with -60° blades wrap angle has the best performance.

3.3 Water head reduction

In the aspects of water head reduction (as shown in Figure 9), models with 120° and -120° blades wrap angles consume more water head than models with 60° and -60° blades wrap angles. The difference in water head reduction is mainly due to the variation of hydraulic loss inside the impellers of different models, which is shown in Figure 10. It can be observed that the hydraulic loss in the impeller reduces with the decrease of blades wrap angle. This is mainly because a bigger blade wrap angle means longer flow channels between blades, which causes severe friction loss when water works on the blades surface. In conclusion, to achieve a good balance between water head

reduction and power output, the model with -60° blades wrap angle has the best performance in this project.

4 CONCLUSIONS

The comparison between simulation and experimental results indicates that both the BEPs of both experimental and simulation results are in the range between 9.5 and $10.5 \text{ m}^3/\text{h}$. Although some deviations exist, the simulation could provide an acceptable prediction of PAT performance.

In addition, four PAT models with different blades wrap angles were built and simulated to compare their performance in terms of both power output and water head reduction. The results show that the blades wrap angle does have effects on the PAT performance. Firstly, the blades wrap angle has an obvious effect on the BEPs. In this study, the best efficiency increases from 12.9% to 16.0% by changing the blades wrap angles and the flow rate at the BEPs also varies. Secondly, the decrease of blades wrap angle may lead to the reduction of hydraulic loss in the impeller, so the total water head reduction will decrease. Thirdly, to achieve a good balance between water head reduction and power output, the model with -60° blades wrap angle has the best performance in this project.

ACKNOWLEDGEMENTS

The authors would like to thank Sino Green Limited (P14-0498) in Hong Kong for funding this project and close collaborations for completing this study.

REFERENCES

- [1] Giosio DR, Henderson AD, Walker JM *et al.* Design and performance evaluation of a pump-as-turbine micro-hydro test facility with incorporated inlet flow control. *Renew Energy* 2015;78:1–6.

- [2] Yang SS, Derakhshan S, Kong F Y. Theoretical, numerical and experimental prediction of pump as turbine performance. *Renew Energy* 2012;**48**:507–13.
- [3] Du J, Yang H, Shen Z *et al.* Micro hydro power generation from water supply system in high rise buildings using pump as turbines. *Energy* 2017;**137**:431–40.
- [4] Yang S, Kong F, Chen B. Research on volute design method of pump as turbine using CFD. *Int Agric Eng J* 2011;**20**:25–32.
- [5] Zhu B, Wang X, Tan L *et al.* Optimization design of a reversible pump–turbine runner with high efficiency and stability. *Renew Energy* 2015;**81**:366–76.
- [6] Singh P, Nestmann F. Internal hydraulic analysis of impeller rounding in centrifugal pumps as turbines. *Exp Therm Fluid Sci* 2011;**35**:121–34.
- [7] Jain SV, Patel RN. Investigations on pump running in turbine mode: a review of the state-of-the-art. *Renew Sust Energ Rev* 2014;**30**:841–68.
- [8] Jain SV, Swarnkar A, Motwani KH *et al.* Effects of impeller diameter and rotational speed on performance of pump running in turbine mode. *Energy Convers Manage* 2015;**89**:808–24.
- [9] Cao K, Yao Z. *The Principle and Hydraulic Design of Water Turbine*. Tsinghua University Press, Beijing, 1991:41–8.
- [10] Yang SS, Kong FY, Shao F *et al.* Numerical simulation and comparison of pump and pump as turbine. *Proc ASME* 2010:141–50.
- [11] Wu J, Shimmei K, Tani K *et al.* CFD-based design optimization for hydro turbines. *J Fluid Eng* 2007;**129**:159–68.
- [12] Croba D, Kueny JL. Numerical calculation of 2D, unsteady flow in centrifugal pumps: impeller and volute interaction. *Int J for Numer Meth Fl* 1996;**22**:467–81.
- [13] Derakhshan S, Nourbakhsh A. Theoretical, numerical and experimental investigation of centrifugal pumps in reverse operation. *Exp Therm Fluid Sci* 2008;**32**:1620–7.
- [14] Zhang B, Liang C. A simple, efficient, and high-order accurate curved sliding-mesh interface approach to spectral difference method on coupled rotating and stationary domains. *J Comput Phys* 2015;**295**:147–60.
- [15] Ferrer E, Willden RHJ. A high order Discontinuous Galerkin–Fourier incompressible 3D Navier–Stokes solver with rotating sliding meshes. *J Comput Phys* 2012;**231**:7037–56.
- [16] Gourdain N. Prediction of the unsteady turbulent flow in an axial compressor stage. Part 1: comparison of unsteady RANS and LES with experiments. *Comput Fluids* 2015;**106**:119–29.
- [17] Coroneo M, Montante G, Paglianti A *et al.* CFD prediction of fluid flow and mixing in stirred tanks: numerical issues about the RANS simulations. *Comput Chem Eng* 2011;**35**:1959–68.
- [18] Liu X, Luo Y, Karney BW *et al.* A selected literature review of efficiency improvements in hydraulic turbines. *Renew Sust Energ Rev* 2015;**51**:18–28.
- [19] Neumann B. The interaction between geometry and performance of a centrifugal pump. Mechanical Engineering Publications, 1991.
- [20] Stepanoff AJ. Centrifugal and axial flow pumps: theory, design, and application, Reprint Edition. 1993.
- [21] Derakhshan S, Nourbakhsh A. Theoretical, numerical and experimental investigation of centrifugal pumps in reverse operation. *Exp Therm Fluid Sci* 2008;**32**:1620–7.